

N. 12-16
020 073

TOWARD OPTIMUM SCALE AND TBC ADHESION ON SINGLE CRYSTAL SUPERALLOYS

James L. Smialek
NASA Lewis Research Center
Cleveland, OH 44135

ABSTRACT

Single crystal superalloys exhibit excellent cyclic oxidation resistance if their sulfur content is reduced from typical impurity levels of ~5 ppmw to below 0.5 ppmw. Excellent alumina scale adhesion was documented for PWA 1480 and PWA 1484 without yttrium additions. Hydrogen annealing produced effective desulfurization of PWA 1480 to ≤ 0.2 ppmw and was also used to achieve controlled intermediate levels. The direct relationship between cyclic oxidation behavior and sulfur content was shown. An adhesion criterion was proposed based on the total amount of sulfur available for interfacial segregation, e.g., ≤ 0.2 ppmw S will maximize adhesion for a 1 mm thick sample. PWA 1484, melt desulfurized to 0.3 ppmw S, also exhibited excellent cyclic oxidation resistance and encouraging TBC lives (10 mils of 8YSZ, plasma sprayed without a bond coat) in 1100°C cyclic oxidation tests.

INTRODUCTION

For many decades the dramatic effects of trace amounts of reactive elements on alumina and chromia scale adhesion has been recognized and widely studied. The connection between scale adhesion and sulfur segregation was reported by Smeggil et al. (1), Lees (2), Luthra and Briant (3), and Ikeda et al. (4), in which strong surface segregation of sulfur occurred from very low levels in the bulk and was curtailed by the addition of reactive elements. Both interface and surface segregation of sulfur has been found on alumina-forming systems (5-9) and for single crystal PWA 1480 and ReneN6 superalloys as well (10,11). Other studies confirmed that adhesion resulted from reducing sulfur (12-16). Discussion of the exact nature of sulfur segregation and its effects on alumina scale growth continues, nevertheless, there is general agreement that reducing the sulfur level produces a first order improvement in scale adhesion in the absence of reactive elements.

Historically, scale adhesion has been effectively achieved by the addition of reactive elements. For many commercial systems relying on protective alumina scales (e.g. polycrystalline NiCrAlY coatings or FeCrAlY heating elements), the direct addition of Y is more practical than removing ppm levels of sulfur. It is assumed that the reactive elements, which are strong sulfide formers, preclude sulfur segregation by bulk gettering (16).

TECHNICAL PUBLICATION APPROVAL FORM

9-23-98

| AUTHOR(S) (Continue in Remarks.) | ORG. CODE | AFFILIATION (See page 2.) | PHONE NO. | MAIL STOP | ROOM NO. |
|----------------------------------|-----------|---------------------------|-----------|-----------|----------|
| James L. Smialek | 5160 | NASA | 5500 | 106-1 | 103 |
| | | | | | |
| | | | | | |
| | | | | | |
| | | | | | |
| | | | | | |

Funding Division No. 5100 Current Funded Task No. YOM 4966 Funding RTOP No. 523-36-13
 Lewis Contract Monitor _____ Org. Code _____ Phone No. _____ Mail Stop _____ Room No. _____
 Contract or Grant No. _____ Other Report No. _____ Non-NASA Funding (Specify) _____
 Contract Organization and Complete Address _____

| | | | | |
|---|--|---|--|--|
| ① REPORT TITLE AND SUBTITLE TOWARD OPTIMUM SCALE AND TBC ADHESION ON SINGLE CRYSTAL SUPERALLOYS | | ② REPORT TYPE (See Page 2 and NPG 2200.2A) <input type="checkbox"/> TP <input type="checkbox"/> Presentation <input type="checkbox"/> TM <input type="checkbox"/> TM or CR <input type="checkbox"/> CR <input type="checkbox"/> No TM or CR (including oral) <input type="checkbox"/> CP <input checked="" type="checkbox"/> Journal article/book <input type="checkbox"/> SP <input type="checkbox"/> Informal STI (Write URL in Remarks.) | | ③ WORK REQUESTED <input type="checkbox"/> Edit <input checked="" type="checkbox"/> Credit only Attach complete report. |
| ④ MEETING TITLE, LOCATION, AND DATE JOURNAL TITLE ELECTROCHEMISTRY SOCIETY SAN DIEGO MAY 3-8 HIGH TEMPERATURE MATERIALS CHEMISTRY (SYMPOSIUM) PUBLISHER/SPONSOR ELECTROCHEMICAL SOCIETY | | ⑤ DISTRIBUTION <input checked="" type="checkbox"/> Standard <input type="checkbox"/> Nonstandard <input type="checkbox"/> Local SECURITY CLASSIFICATION <input checked="" type="checkbox"/> Unclassified <input type="checkbox"/> Confidential <input type="checkbox"/> Secret Patent Notice given to authors: Initials _____ Date ____/____/____ | | |
| ⑦ TRADE NAMES USED? <input checked="" type="checkbox"/> Yes <input type="checkbox"/> No | | ⑧ SUBJECT CATEGORY(IES) | | |
| ⑨ SUBJECT TERMS (From NASA Thesaurus) | | ⑥ DISTRIBUTION AVAILABILITY CATEGORY (See NPG 2200.2A) <input type="checkbox"/> No Restriction <input type="checkbox"/> Export Controlled <input checked="" type="checkbox"/> Publicly available <input type="checkbox"/> ITAR - USML Category No. _____ <input type="checkbox"/> Publicly available SBIR (attach letter) <input type="checkbox"/> Confidential Commercial <input type="checkbox"/> EAR - ECCN _____ <input type="checkbox"/> Trade secret <input type="checkbox"/> Patent <input type="checkbox"/> License Agreement <input type="checkbox"/> Space Act Agreement (SAA) No. _____ <input type="checkbox"/> LERD <input type="checkbox"/> Copyrighted <input type="checkbox"/> SBIR Restricted until ____/____/____ Availability for restricted document <input type="checkbox"/> U.S. Government Agencies and U.S. Government Agency Contractors Only <input type="checkbox"/> NASA Contractors and U.S. Government Agencies Only <input type="checkbox"/> U.S. Government Agencies Only <input type="checkbox"/> NASA Personnel and NASA Contractors Only <input type="checkbox"/> NASA Personnel <input type="checkbox"/> Available Only with Approval of Issuing Office (Program Office or NASA Center) Limited until ____/____/____ (if applicable) | | |
| Approvals must be complete before your report can be processed. | | | | |
| ⑩ MANAGEMENT REVIEWS AND APPROVALS Initial Date Author/Technical Monitor name (printed) James L. Smialek JLS 5/14/98 Branch Chief/Office Head name (printed) Leslie A. Greenbauer-Seng LAS 5/19/98 Division Chief name (printed) _____ Editing waived? <input type="checkbox"/> Yes <input type="checkbox"/> No TECHNICAL REVIEW COMMITTEE (Required for standard distribution reports.) Chair or Reviewer name (printed) _____ Checker name (printed) (Doug Ming Zhu) Advisor name (printed) _____ | | | | |
| ⑪ DISTRIBUTION REVIEWS AND APPROVALS Author/Originator name (printed) Signature Date Branch Chief name (printed) L.A. Greenbauer-Seng J.L. Greenbauer 5-19-98 Division Chief name (printed) _____ Intellectual Property Officer name (printed) (if required) _____ Center Export Administrator name (printed) _____ | | | | |

REMARKS

Recent single crystal superalloys have become very oxidation resistant, due in part to high aluminum and refractory metal contents. This has allowed the manifestation of a strong reactive metal dopant effect. Hf additions present in PWA 1484, Rene'N5' and CMSX 4, do not appear as potent as Y in imparting scale adhesion. Unfortunately, the desired level of Y (0.01 to 0.1%) is not easily achieved in advanced single crystal superalloys. Nonuniform Y distributions and Y reactions with mold materials during crystal growth present serious casting difficulties. Thus an alternative approach would be to produce low sulfur components through strictly controlled raw materials, melting and casting procedures. Indeed many previous studies have verified improved cyclic oxidation resistance as the sulfur content was reduced below 1 ppmw. The acceptable sulfur level is thus an important quantity to define.

This paper addresses the concept of a critical sulfur content, i.e., the maximum tolerable without degrading scale adhesion. To this end, the oxidation behavior of superalloys is described as a function of various sulfur contents, as controlled by a laboratory hydrogen annealing process. The success of this process was first demonstrated for PWA 1480, annealed in 1 atm hydrogen at 1200° and 1300°C by Tubbs and Smialek (17,18).

EXPERIMENTAL PROCEDURE

The samples tested were obtained from polycrystalline bar stock of PWA 1480, electrodischarge machined to 12 x 25 mm coupons that were 0.2, 0.4, 1.2, 2.5, or 5 mm thick. These were polished through 600 grit emery, cleaned in detergent, and rinsed in ethanol. The starting sulfur content was determined to be about 6.2 ppmw by GDMS, (glow discharge mass spectroscopy). Hydrogen annealing was performed in a flowing 5% H_2 /Ar mixture in high purity alumina tubes. Times and temperatures varied from 8-100 hr and 1000°C to 1300°C, respectively. All samples appeared clean and metallic, with less than ± 0.03 mg/cm² weight change after annealing. Cyclic oxidation was performed in air in a vertical tube furnace, with automatic timers, counters, and pneumatic actuators. The test temperature was 1100°C (2012°F), with 1 hr. heating and 10 min. cooling each cycle. The samples were weighed at various intervals up to 1000 hr. Scales were characterized by x-ray diffraction and SEM.

RESULTS AND DISCUSSION

Hydrogen Annealing. The desulfurization of metals by hydrogen annealing has been assumed to be a diffusion controlled surface segregation process (17), in which rapid cleaning occurs by sulfur evaporation or formation of H_2S gas. Hydrogen atmospheres prevent alumina scale formation, which would otherwise obstruct the removal of sulfur. The effect of annealing time, temperature, and thickness on the resulting average sulfur content is shown in figure 1. (Thickness plays an additional role in defining a critical sulfur content, as will be describe later). Assuming diffusion control of desulfurization, the thin slab diffusion solution provides the following approximation for values of $Dt/L^2 > 0.05$:

$$C/C_0 = 8/\pi^2 \exp(-\pi^2 D_s t/L^2) \quad [1]$$

where C_t and C_o are the final and original average sulfur contents, D_s is the diffusion coefficient of sulfur in nickel, t is time, and L is thickness (17,18). The measured (filled bars) and projected from eqn. 1 (hashed bars) average sulfur contents for some of the test matrix conditions are shown in figure 1, for a starting level of 6.2 ppmw. There is general agreement in the overall exponential desulfurization trends with increasing time and diffusivity (temperature) and with increasing thickness. It can be seen that sulfur levels below 0.2 ppmw have been achieved for a number of the exposure conditions.

Gravimetric Data. The effect of annealing conditions on the 1100°C cyclic oxidation weight change curves is shown in figure 2-4. In figure 2, the effect of annealing temperature is shown for 0.5 mm (20 mils) samples annealed for 20 hr. Under these conditions, the 1000° and 1100° C anneals did little to improve the cyclic oxidation resistance over that of the as-received (unannealed) control sample. The latter three conditions exhibited more than 20 mg/cm² weight loss after 500 1-hr cycles. The 1200° and 1300°C annealing treatments, however, resulted in 500 hr weight changes of +0.58 and -0.82 mg/cm², respectively. This represents a very significant improvement. (It should be noted that the degradation of the 1300°C sample was related to the partial melting that occurred upon annealing and attendant modification of oxidation behavior).

The effect of annealing time on oxidation is shown in figure 3 for 0.5 mm samples annealed at 1200°C. Here a significant improvement was noted by only an 8 hr anneal, producing a moderate weight loss of 6.7 mg/cm² after 1000 hr. Furthermore, the 1000 hr weight changes of the 20, 50, and 100 hr samples were all excellent (+0.10, +0.36, and +0.16 mg/cm², respectively).

The effect of sample thickness on oxidation is shown in figure 4 for samples annealed at 1200°C for 100 hr. While the 500 hr. weight change for 5 and 2.5 mm samples (-13.8 and -5.7 mg/cm²) was not as severe as that for unannealed samples (-33 to -67 mg/cm²), more significant improvement resulted for 1.3, 0.5 and 0.25 mm samples (0.75, 0.58, and 0.65 mg/cm²).

X-ray Diffraction. Scale phases were identified from X-ray diffractometer scans. The major phases were Al₂O₃, Ni(Al,Cr)₂O₄, and CrTaO₄ after 500 hr of cycling. A greater relative amount of Al₂O₃ was noted for the more oxidation resistant samples, and more NiCr₂O₄ and CrTaO₄ for the samples with poor scale adhesion. This is substantially the same result obtained previously for hydrogen annealed PWA 1480 (18).

Effect of Sulfur Content. The 500 hr weight change of the 0.5 mm samples tested is shown in figure 5 as function of the measured sulfur content. The sulfur level of the 1000° and 1100°C annealed samples was 4 and 2 ppmw and the performance of these samples was only marginally improved. The sulfur level of the sample annealed at 1200°C for 8 hr was 0.8 ppmw, and its performance was notably improved. Finally, the annealing treatments for longer times or higher temperatures produced excellent behavior for sulfur contents of 0.05 to 0.3 ppmw. In order to resolve a critical sulfur content (below which no further improvement in cyclic oxidation is achieved), a value corresponding to 0.0 mg/cm² weight change after 500 hr was interpolated as ~ 0.4 ppmw S. Similarly, the sulfur value corresponding to the onset of severe spallation (defined as -10.0 mg/cm² weight change) was 1.2 ppmw S. This procedure was performed for each sample thickness.

These two interpolated boundaries are shown on the adhesion map of figure 6, where alloy sulfur content is plotted against sample thickness with log-log axes. Thus samples with sulfur contents below the 0.0 mg/cm^2 boundary exhibit adherent behavior and those having sulfur contents above the -10.0 mg/cm^2 boundary are approaching the least adherent behavior. Alternatively, the behavior of specific samples is indicated by the individual data points. Here the degree of shading relates to the degree of adhesion as defined by the side legend.

It is believed that the defining boundaries exhibit a negative slope and thicker samples will require lower levels of sulfur to achieve the equivalent degree of adhesion. (A more precise slope is not claimed because of some variation in sulfur measurements, especially at values less than 0.5 ppmw). This trend is expected because of the greater amounts of total sulfur available for repeated segregation and scale spallation for thicker samples.

Adhesion Criteria. A more fundamental approach has also been suggested to define a critical sulfur content (13). This concept holds that the limit of an adhesion benefit would be obtained if the sample contains a total amount of sulfur less than that required to produce 1 monolayer of segregation. The implication is that a fraction of a monolayer is required to cause a significant spallation event; but with only limited replenishment, it is unable to sustain repetitive degradation. The equivalence between bulk and segregated sulfur was approximated as:

$$C_s = (8.27 \times 10^{-2} \text{ gm/cm}^2) * N_m A / W \quad (13) \quad [2]$$

where: C_s = bulk sulfur content in ppmw
 N_m = number of segregated monolayers
 A = sample surface area in cm^2
 W = sample weight in gm

The 1 monolayer criterion is shown on figure 6 for PWA 1480 coupons of density 8.72 gm/cm^3 . All conditions above this line contain more than the indicated 1 monolayer of sulfur; all those below contain less than 1 monolayer. Note that this criterion is close to the interpolated experimental boundary for adhesion. The boundary for nonprotective behavior corresponds to about 4 monolayers of total sulfur available for segregation. This behavior is similar to that observed for Rene' N5 and summarized for other similar studies (18,19).

TBC performance. Melt desulfurized PWA 1484, which does contains 0.1% Hf, was obtained with 0.3 ppmw S (courtesy of L. Graham, PCC Airfoils, Inc.). The cyclic oxidation resistance is shown in figure 7 and indicates excellent behavior for at least 2000 hr. Also no appreciable difference exists between as-received samples and those hydrogen annealed at 1250°C for 50 hr. This excellent behavior warranted an exploratory study on TBC coatings without bondcoats. About $250 \mu\text{m}$ of 8YSZ was plasma sprayed onto melt desulfurized PWA 1484 (at 40 kW, 10 cm spray distance, $50 \mu\text{m}$ per pass, 250°C substrate temperature). The oxidation behavior of three processing versions are shown as samples A, B, and C in figure 8. Arrows indicate observations of cracks or small delaminations, while the large vertical weight drops indicate TBC spallation, usually as one, free-standing piece, consisting of the entire side. While the bondcoat system possessed the longest life for complete detachment, serious edge delamination cracks began growing in about the same time frame that the no-bondcoat systems exhibited distress. A higher oxidation rate of the APS NiCrAlY bondcoat is also evident.

The no-bondcoat failure surfaces exhibited blue particles on the YSZ coating underside, identified as NiAl_2O_4 spinel by XRD. Conversely, the exposed metal side exhibited some tetragonal YSZ particles on the blue spinel-covered surface, with an $\alpha\text{-Al}_2\text{O}_3$ inner scale. Very little spalling to bare metal was observed. Since the failure locus was at the spinel-YSZ interface, the $\alpha\text{-Al}_2\text{O}_3$ scale adhesion appeared adequately strong under these conditions.

CONCLUDING REMARKS

This summary has shown the strong dependence of single crystal superalloy oxidation resistance on low levels of sulfur impurity contents. Extraordinary improvements are possible from desulfurization by hydrogen annealing. Typical sample thicknesses ~ 1 mm may be easily desulfurized to < 1 ppmw by annealing at 1200°C . Sulfur segregation in hydrogen annealed superalloys is essentially eliminated. This in turn produces excellent cyclic oxidation behavior at $1100^\circ\text{--}1150^\circ\text{C}$ with very small weight changes of only 0.5 to 1 mg/cm^2 after 1000 hours. Both empirical and fundamental criteria of scale adhesion suggest that a critical sulfur content of 0.1-1 ppmw is required to obtain the maximum adhesion, depending on sample thickness. A first attempt at TBC coating a low sulfur superalloy without a bond coat provided appreciable lives without failure at the oxide-metal interface.

REFERENCES

1. J.G. Smeggil, A.W. Funkenbusch, and N.S. Bornstein, *Metall. Trans.*, 17A, 923, (1986).
2. D.G. Lees, *Oxidation of Metals*, 27, 75, (1987)
3. K.L. Luthra and C.L. Briant, Fundamental Aspects of High Temperature Corrosion - II, D. Shores, G. Yurek, eds., The Electrochemical Society, Pennington, NJ, 86-9, p.187 (1986).
4. Y. Ikeda, K. Nii, and K. Yoshihara, Proceedings JIMIS-3: High Temperature Corrosion Transactions of the Japan Institute of Metals, Supplement 24, p.207 (1983).
5. J.L. Smialek and R. Browning, High Temperature Materials Chemistry III, R. Rapp, ed., The Electrochemical Society, Pennington, NJ, p. 259 (1986).
6. C.G.H. Walker and M.M. El Gomati, *Appl. Surf. Sci.*, 35, 164, (1988-89).
7. P.Y. Hou and J. Stringer, *Oxidation of Metals*, 38, 323, (1992).
8. H.J. Grabke, G. Kurbatov, and H.J. Schmutzler, *Oxidation of Metals*, 43, 97 (1995).
9. P.Y. Hou, *This Proceedings*, The Electrochemical Society, Pennington, NJ, (1998).
10. D.T. Jayne and J.L. Smialek, Microscopy of Oxidation, 2, S.B. Newcomb and M.J. Bennett, eds, The Institute of Metals, p.183 (1993).
11. M.A. Smith, W.E. Frazier, and B.A. Pregger, *Mat. Sci. and Engineer.*, 203, 388, (1995).
12. J. G. Smeggil, *Mater. Sci. and Engineer.*, 87, 261, (1987).
13. J.L. Smialek, *Metall. Trans.*, 22A, 739, (1991).

14. R.V. McVay, P. Williams, G.H. Meier, F.S. Pettit, and J.L. Smialek, Superalloys 1992, S.D. Antolovich et al., eds., TMS-AIME, Warrendale, PA, 807, (1992).
15. T.A. Kircher, A.Khan, and B. Pregger, paper presented at Aeromat 91, Long Beach, CA, ASM, (1991).
16. G.H. Meier, F.S. Pettit, and J.L. Smialek, *Werkstoffe und Korrosion*, 46, 232 (1995).
17. B.K. Tubbs and J.L. Smialek, Corrosion and Particle Erosion at High Temperatures, V. Srinivasan and K. Vedula, eds., TMS-AIME, Warrendale, PA, 459, (1989).
18. J.L. Smialek and B.K. Tubbs, *Metall. and Mat. Trans.*, 26A, 427, (1995).
19. J.L. Smialek, D.T. Jayne, J.C. Schaeffer, and W.C. Murphy, *Thin Solid Films*, 253, 285 (1994).
20. J.L. Smialek, *J. Engineer. Gas Turbine Power*, 2, 370, (96-GT-519), (1998).

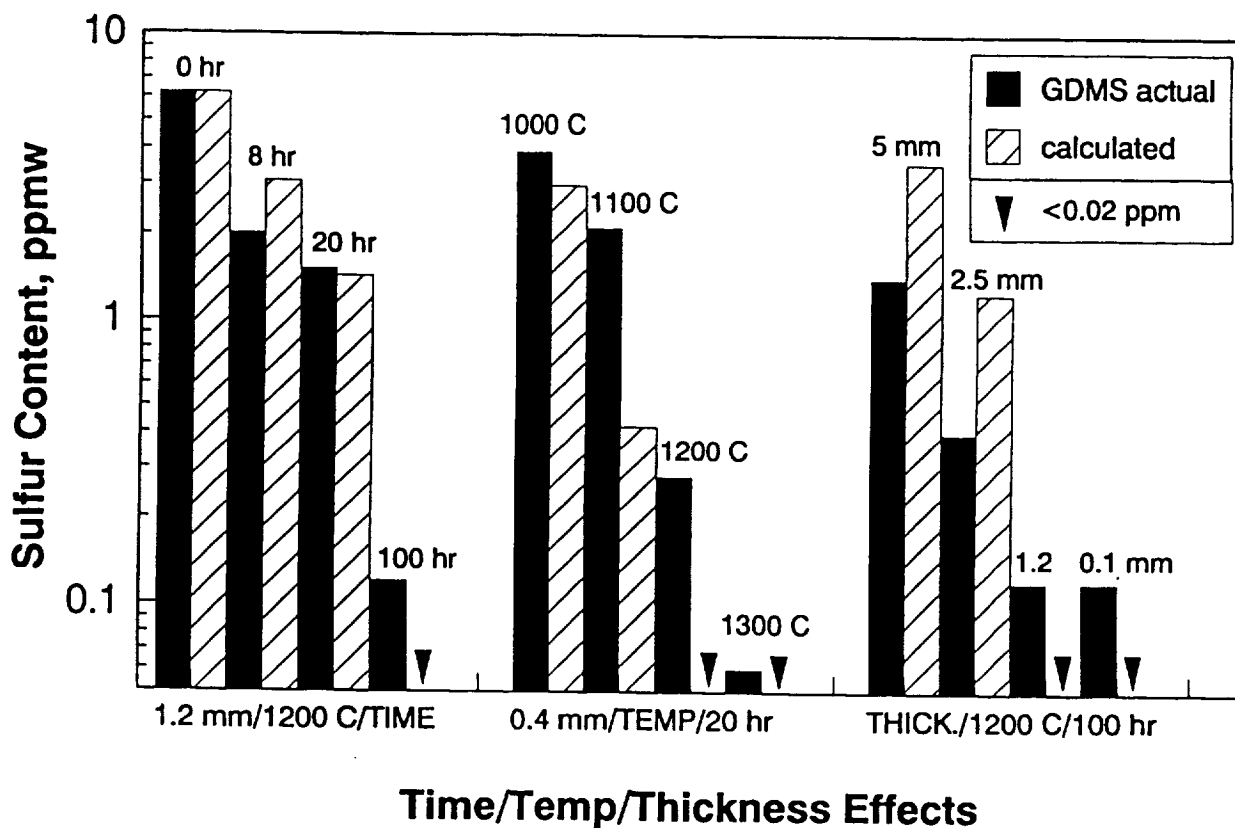


Figure 1. Effect of hydrogen annealing parameters on desulfurization of PWA 1480.

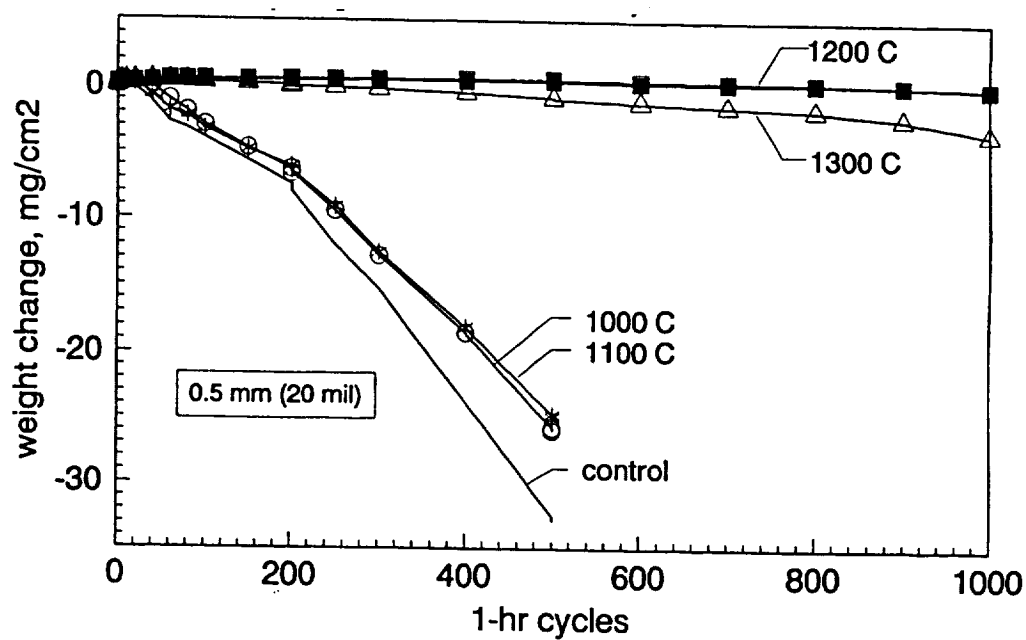


Figure 2. Effect of hydrogen annealing temperature (for 20 hr anneals) on the 1100°C cyclic oxidation behavior of 0.5 mm PWA 1480 samples.

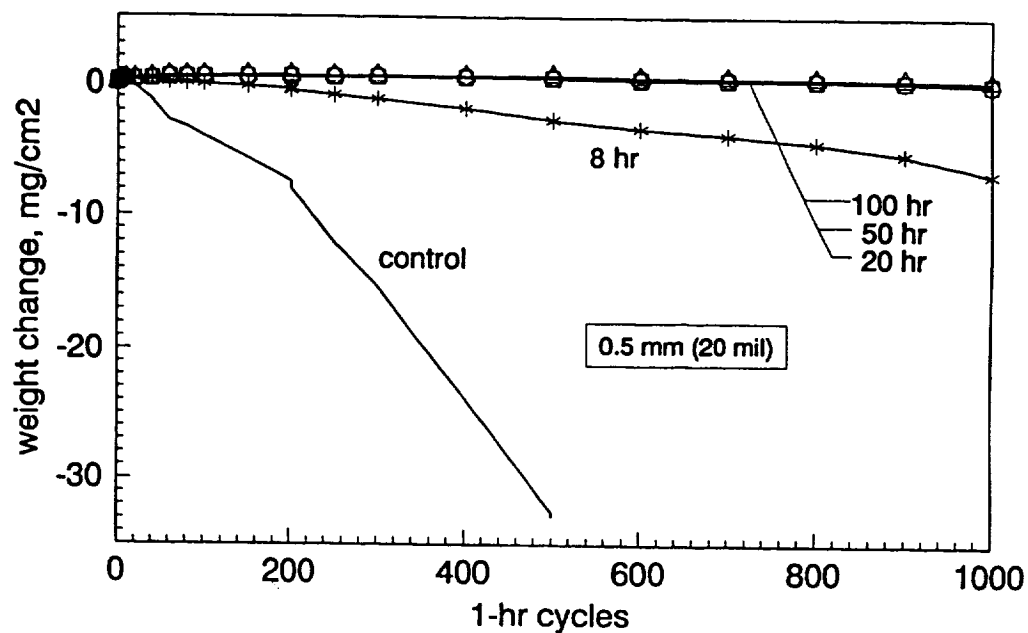


Figure 3. Effect of hydrogen annealing time (for 1200°C anneals) on the 1100°C cyclic oxidation behavior of 0.5 mm PWA 1480 samples.

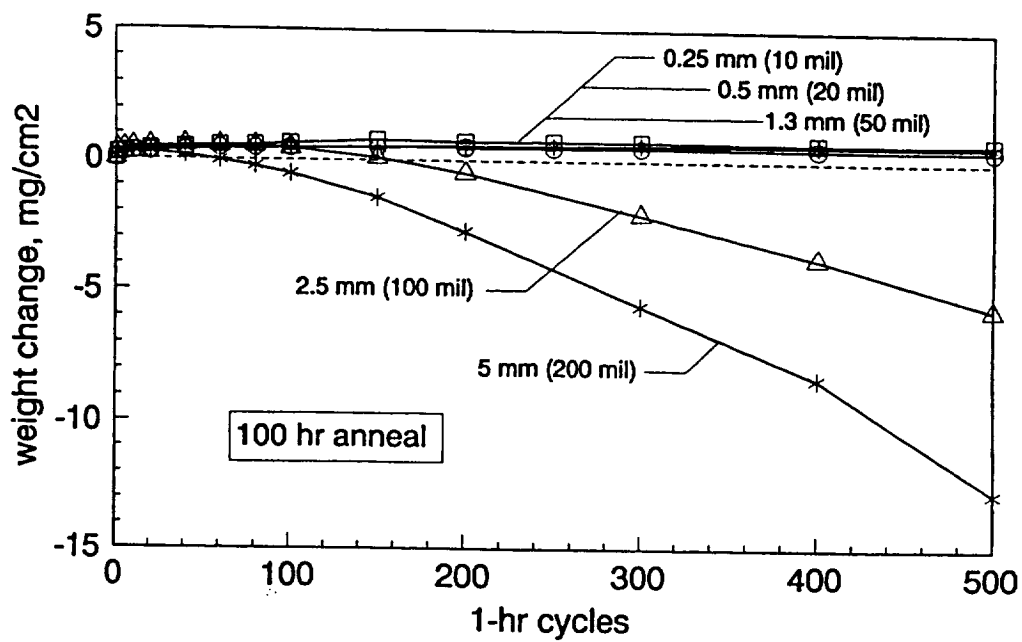


Figure 4. Effect of sample thickness (hydrogen annealed for 100 hr at 1200°C) on the 1100°C cyclic oxidation behavior of PWA 1480 samples.

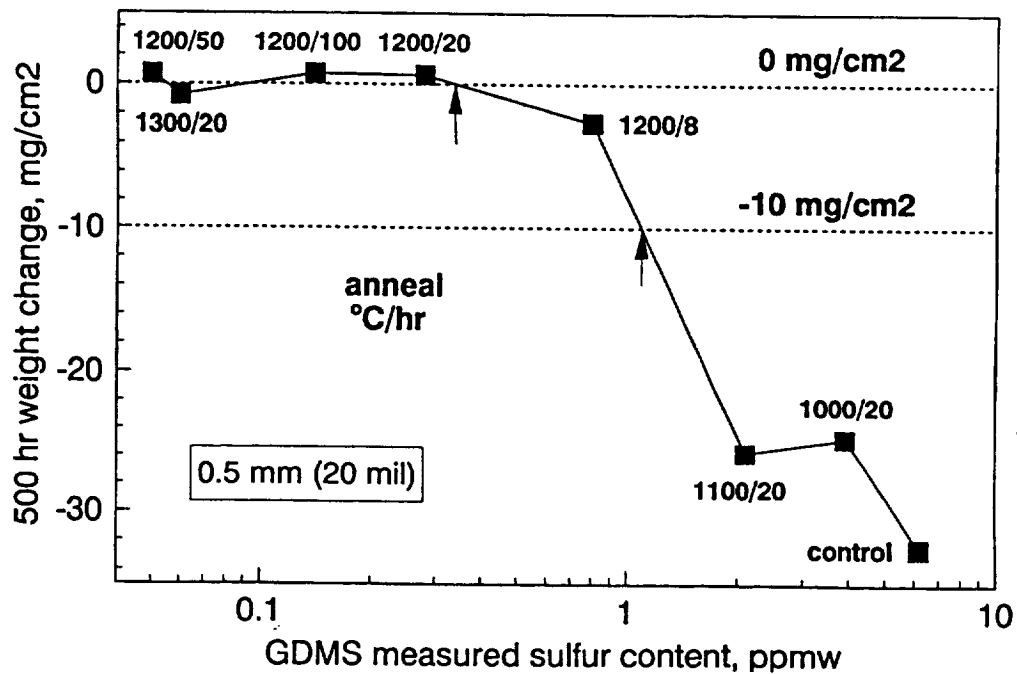


Figure 5. Relationship between weight change after cyclic oxidation for 500 hr at 1100°C and sulfur content of 0.5 mm samples that were hydrogen annealed under various conditions.

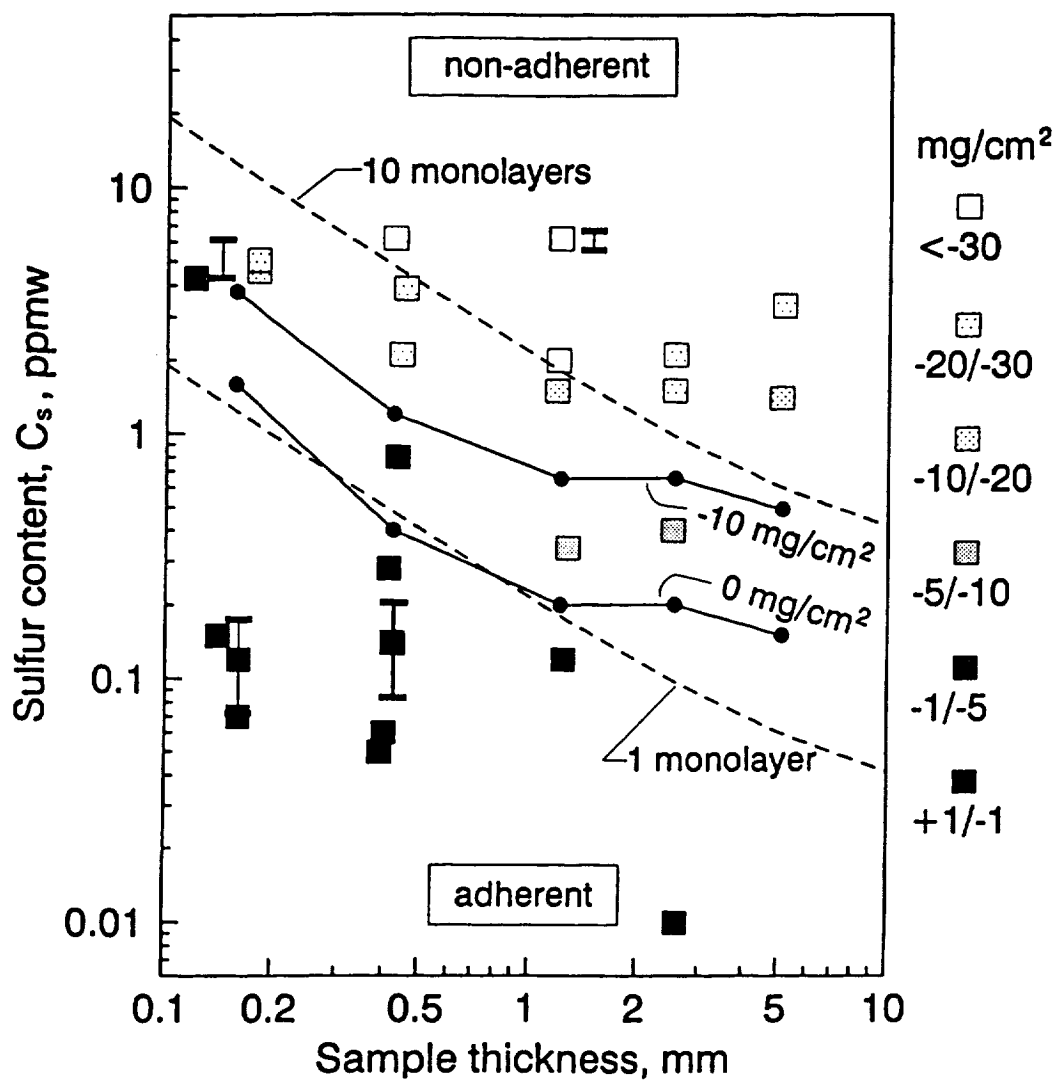


Figure 6. Adhesion map showing critical sulfur content based on experimental interpolation (0.0 and -10 mg/cm² weight change at 500 hr.) and proposed 1 monolayer segregation criterion. Symbols represent actual data; degree of shading indicates degree of adhesion according to legend.

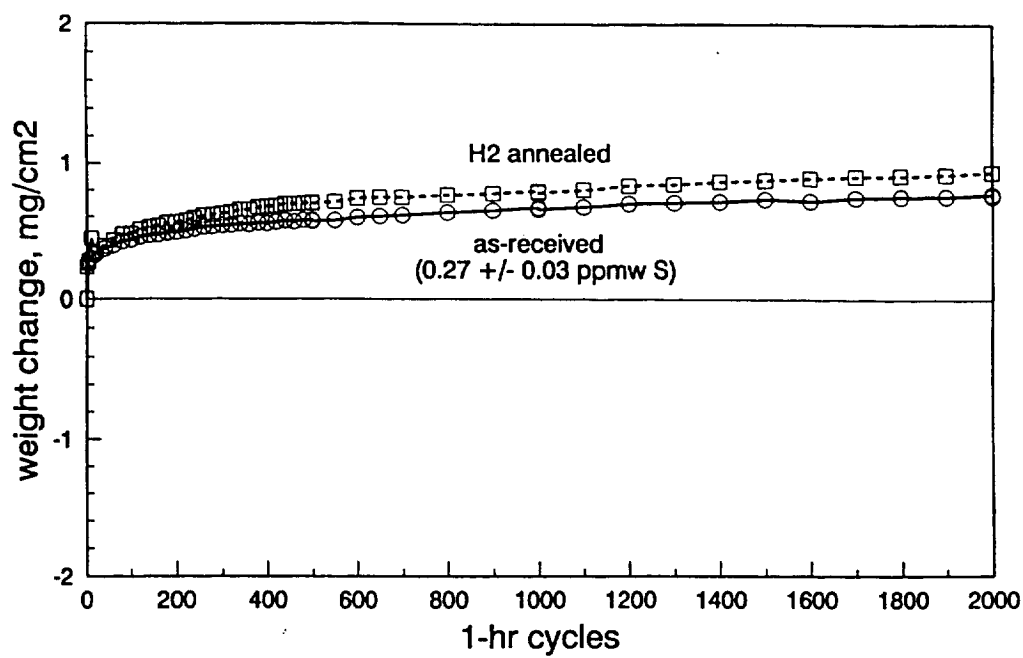


Figure 7. 1100°C cyclic oxidation behavior of PWA 1484 melt desulfurized to 0.3 ppmw S.

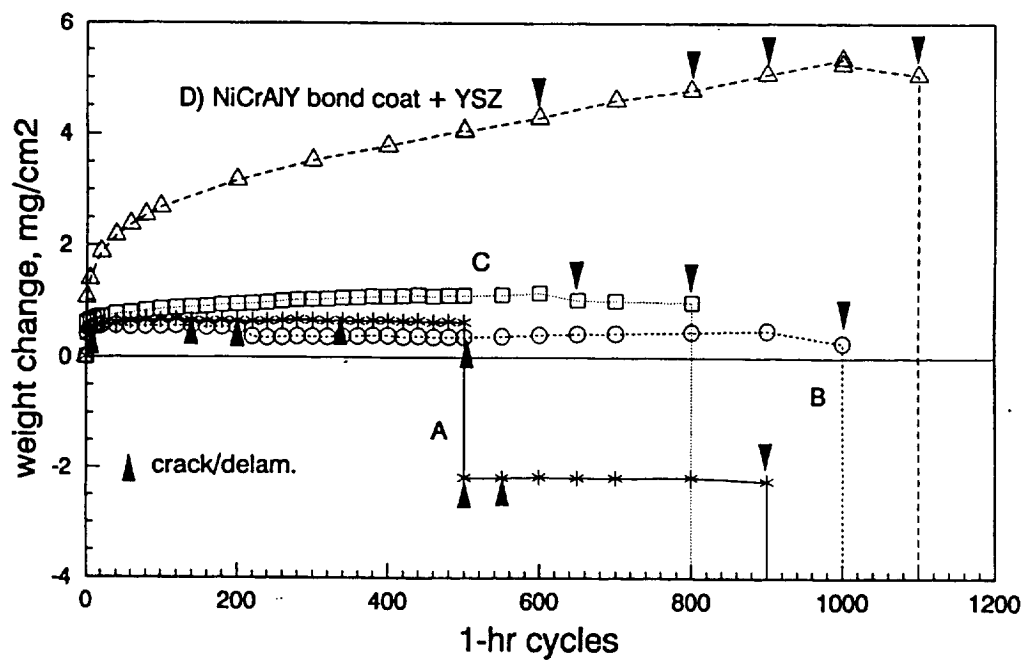


Figure 8. 1100°C cyclic oxidation behavior of plasma sprayed 250 µm 8YSZ TBC on melt desulfurized PWA 1484 (no bondcoat compared to 125 µm APS NiCrAlY bondcoat).

